Transp Porous Med (2008) 71:133–145
DOI 10.1007/s11242-007-9114-7

Double diffusive convection of anomalous density fluids in a porous cavity

S. Sivasankaran · P. Kandaswamy · C. O. Ng

Received: 6 October 2006 / Accepted: 11 February 2007 / Published online: 6 April 2007

Abstract A numerical study has been performed to analyze the combined effect of temperature and species gradients on the buoyancy-driven natural convection flow of cold water near its density extremum contained in a porous cavity. The governing equations are descretized using the finite volume method. The results of the investigation are presented in the form of steady-state streamlines, velocity vectors, isotherms, and isoconcentrationlines. The results are discussed for different porosities, Darcy numbers, and Grashof numbers. The heat and mass transfer rates calculated are found to behave nonlinearly with hot wall temperature. The heat and mass transfer are increased with increasing Darcy number and porosity. It is found that the convective heat and mass transfer rate are greatly affected by the presence of density maximum.

Keywords Natural convection · Density maximum · Porous medium

1 Introduction

Natural convection of cold water in enclosures has been studied extensively in the past due to the fact that this phenomenon plays an important role over a wide range of occurrences in nature and technology, Nield and Bejan (2006). Vafai (2005) gives a deep insight into convective heat transfer in porous media. The operation of PEM fuel cell involves heat and mass transfer in porous media. In PEM Fuel cell, the cathode region is saturated with water and chemicals thus forming fluid saturated porous media, Barbir (2005). In this situation, the study of heat and mass transfer in porous media assumes significance in industrial, engineering,

S. Sivasankaran · P. Kandaswamy (✉)
Department of Mathematics, UGC DRS Centre for Fluid Dynamics, Bharathiar University, Coimbatore, India
e-mail: pgkswamy@yahoo.co.in

C. O. Ng
Department of Mechanical Engineering, The University of Hong Kong, Pokfulam Road, Hong Kong, Hong Kong

and technology, Sunden and Faghri (2005). Water possesses a maximum density near 4°C. Due to the effect of density inversion, convection of water behaves in a complicated manner. Mehta and Nandakumar (1987) investigated the natural convection heat and mass transfer in non-homogeneous porous medium and found that vigorous convection through high permeability regions make the temperature and concentration in the porous layer quite different from that of the homogeneous case.

Weiss et al. (1991) investigated the effect of water density extremum on heat transfer within a cylinder containing a heat generating porous media. They found that conduction was the dominant mode of heat transfer at the low heat generation rate. A numerical study on double diffusive convection in a fluid saturated porous enclosure by Mamou et al. (1995) showed that the flow is solutally driven when Lewis number is small and thermally driven when it is sufficiently large for constant value of thermal Darcy–Rayleigh number. Goyeau et al. (1996) numerically investigated the double diffusive natural convection in a porous cavity using Darcy–Brinkman model. They found the numerical results for mass transfer to be in good agreement with the results of scaling analysis over a very wide range of parameters.

Nithiarasu et al. (1997) numerically studied the double diffusive natural convection in a fluid saturated porous cavity. Their results showed that the flow, heat and mass transfer become sensitive to applied mass transfer coefficient. They also observed that the Sherwood number approaches a constant value as the solutal Biot number increases. Sundaravadivelu and Kandaswamy (2000) analyzed natural convection flow of pure water around its temperature of maximum density by using a non-linear temperature dependent equation for density in a square cavity.

Zheng et al. (2001) numerically studied convection in a cavity filled with porous medium saturated with water near 4°C. They found that the symmetry of flow and temperature fields observed for the isotropic porous medium at density inversion parameter is unity. Benhadji et al. (2002) studied convection in a porous cavity saturated with water near 4°C. They found that the presence of two convective cells of equal intensity results in a much less efficient heat transfer mechanism.

Considerable number of numerical studies concerning the double diffusive convection in porous enclosures in the past are typically devoted to a linear density temperature dependent fluid. For a number of fluids like water, antimony, sodium, bismuth, and tolurium, the density–temperature relation exhibits an extremum. Since the coefficient of thermal expansion changes sign at this extremum, simple linear relations for density as a function of temperature are inadequate near the extremum and hence Sivasankaran and Kandaswamy (2006) studied double diffusive convection of water near its density maximum in rectangular cavities using non-linear density–temperature relation of Kandaswamy and Kumar (1999). In this study keeping these in mind we study double diffusive convection of fluids with nonlinear density–temperature relation in fluid saturated porous cavity.

2 Mathematical formulation

Consider a two-dimensional square cavity of side L with water saturated porous medium as shown in Fig. 1a. The vertical isothermal sidewalls of the cavity are maintained at different temperatures θ_h and θ_c, where $\theta_h > \theta_c$. The concentration level of mass is taken to be c_2 at $y = 0$ and c_1 at $y = L$, where $c_1 > c_2$. The horizontal walls are thermally insulated. The gravity acts in the downward direction. The velocity components u and v are taken in the x and y directions, respectively. The porous medium is assumed to be isotropic,

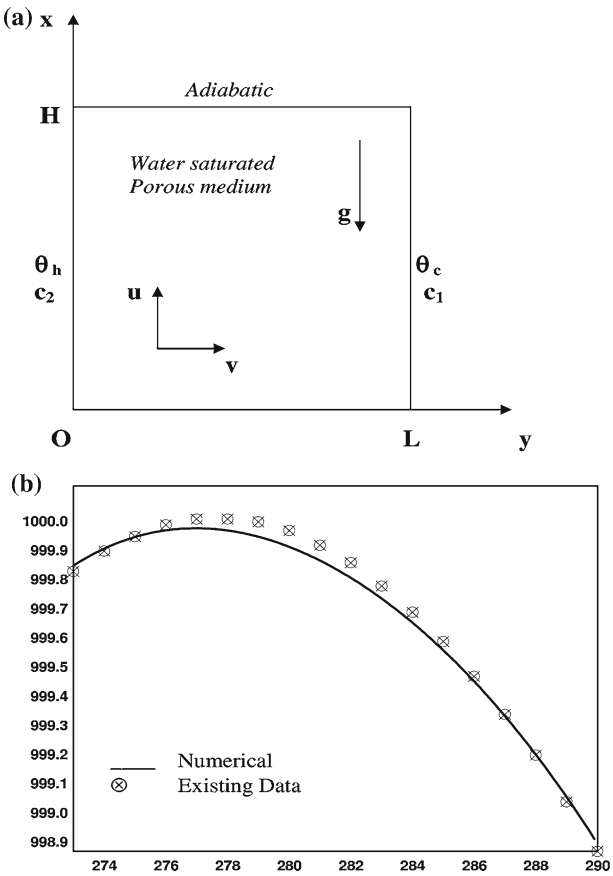

Fig. 1 (**a**) Physical configuration. (**b**) Density vs. temperature.

homogeneous, and in thermodynamic equilibrium with the fluid, which is Newtonian and incompressible. The Brinkman Forchheimer extended Darcy model is used, Nithiarasu et al. (1997) and Khanafer and Vafai (2002). The thermal properties of the fluid are constant and specific heat ratio (σ) is assumed to be one, Khanafer and Vafai (2002). In the past many correlations have been proposed to represent the density of cold water as a function of temperature such as rational function or polynomial approximation. Most of the authors like Poulikakos (1984), Lin and Nansteel (1987) and Ho and Lin (1990) have used a parabolic relation for density as $\rho = \rho_o \left[1 - \beta(\theta - \theta_c)^2\right]$. But this relation is valid only in the temperature range between 0° and 8°. Since this relation is not valid above the temperature of 8°, a fourth order polynomial of the form $\rho = \rho_o \left[1 - \left(\sum_{i=1}^{4}(-1)^i \beta_i (\theta - \theta_c\right)^i - \beta_5(c - c_2))\right]$, Sundaravadivelu and Kandaswamy (2000), is used where $\rho_0 (= 999.84)$ is the density of water at θ_c and $\beta_1 = 6.8143 \times 10^{-5}$, $\beta_2 = 9.9901 \times 10^{-6}$, $\beta_3 = 2.7217 \times 10^{-7}$, $\beta_4 = 6.7252 \times 10^{-9}$, and $\beta_5 = 3.0 \times 10^{-3}$. See also, Vasseur et al. (1983), Gobin and Bennacer (1996). The graph for above relation agrees with the plot for data available, see Fig. 1b.

The equations governing the motion specified as above are

$$\frac{\partial u}{\partial x}+\frac{\partial u}{\partial y}=0 \tag{1}$$

$$\frac{1}{\epsilon}\frac{\partial u}{\partial t}+\frac{1}{\epsilon^2}\left[u\frac{\partial u}{\partial x}+v\frac{\partial u}{\partial y}\right]=-\frac{1}{\rho_o}\frac{\partial p}{\partial x}+\frac{\nu}{\epsilon}\left[\frac{\partial^2 u}{\partial x^2}+\frac{\partial^2 u}{\partial y^2}\right]-\frac{\nu}{K}u - \frac{1.75}{\sqrt{150}\epsilon^{3/2}}\frac{u\sqrt{u^2+v^2}}{\sqrt{K}}-\frac{\rho}{\rho_o}g \tag{2}$$

$$\frac{1}{\epsilon}\frac{\partial v}{\partial t}+\frac{1}{\epsilon^2}\left[u\frac{\partial v}{\partial x}+v\frac{\partial v}{\partial y}\right]=-\frac{1}{\rho_o}\frac{\partial p}{\partial y}+\frac{\nu}{\epsilon}\left[\frac{\partial^2 v}{\partial x^2}+\frac{\partial^2 v}{\partial y^2}\right]-\frac{\nu}{K}v - \frac{1.75}{\sqrt{150}\epsilon^{3/2}}\frac{v\sqrt{u^2+v^2}}{\sqrt{K}} \tag{3}$$

$$\sigma\frac{\partial \theta}{\partial t}+u\frac{\partial \theta}{\partial x}+v\frac{\partial \theta}{\partial y}=\alpha\left[\frac{\partial^2 \theta}{\partial x^2}+\frac{\partial^2 \theta}{\partial y^2}\right] \tag{4}$$

$$\epsilon\frac{\partial c}{\partial t}+u\frac{\partial c}{\partial x}+v\frac{\partial c}{\partial y}=D\left[\frac{\partial^2 c}{\partial x^2}+\frac{\partial^2 c}{\partial y^2}\right] \tag{5}$$

where θ is the temperature of the fluid, c is the species concentration in the fluid, K is the permeability of the porous medium, ρ is the density, p is the pressure, α is the thermal diffusivity, D is the species diffusivity, ϵ is the porosity, $\sigma(=1)$ is the specific heat ratio and ν is the kinematics viscosity of the fluid.

The appropriate initial and boundary conditions are

$$\begin{array}{lll} t=0: & u=v=0, & \theta=\theta_c, c=c_2, \quad 0\le x\le L, 0\le y\le L \\ t>0: & u=v=0, & \frac{\partial\theta}{\partial x}=\frac{\partial c}{\partial x}=0, \quad x=0\&L \\ & u=v=0, & \theta=\theta_h, c=c_2 \quad y=0 \\ & u=v=0, & \theta=\theta_c, c=c_1 \quad y=L. \end{array}$$

The non-dimensional variable are introduced as follows

$$X=\frac{x}{L},\quad Y=\frac{y}{L},\quad U=\frac{u}{\nu/L},\quad V=\frac{v}{\nu/L},\quad \tau=\frac{t}{L^2/\nu},\quad \Psi=\frac{\psi}{\nu},$$
$$\zeta=\frac{\omega}{\nu/L^2},\quad T=\frac{\theta-\theta_c}{\theta_h-\theta_c}\quad C=\frac{c-c_2}{c_1-c_2}.$$

The vorticity stream function formulation of the problem (1)–(5) in non-dimensional form can be written as

$$\frac{1}{\epsilon}\frac{\partial \zeta}{\partial \tau}+\frac{1}{\epsilon^2}\left[-\frac{\partial \Psi}{\partial Y}\frac{\partial \zeta}{\partial X}+\frac{\partial \Psi}{\partial X}\frac{\partial \zeta}{\partial Y}\right]=\frac{1}{\epsilon}\nabla^2\zeta-\frac{1}{Da}\zeta-\frac{Fc\zeta}{\sqrt{Da}} - \frac{Fc}{Da|\mathbf{v}|^2}\left[\frac{\partial \Psi}{\partial Y}\frac{\partial |\mathbf{v}|^2}{\partial Y}+\frac{\partial \Psi}{\partial X}\frac{\partial |\mathbf{v}|^2}{\partial X}\right]-\sum_{i=1}^{4} i(-1)^i Gr_i^T T^{(i-1)}\frac{\partial T}{\partial Y}+Gr_5^C\frac{\partial C}{\partial Y} \tag{6}$$

$$\zeta=-\nabla^2\Psi \tag{7}$$

$$\sigma \frac{\partial T}{\partial \tau} - \frac{\partial \Psi}{\partial Y}\frac{\partial T}{\partial X} + \frac{\partial \Psi}{\partial X}\frac{\partial T}{\partial Y} = \frac{1}{Pr}\nabla^2 T \tag{8}$$

$$\epsilon \frac{\partial C}{\partial \tau} - \frac{\partial \Psi}{\partial Y}\frac{\partial C}{\partial X} + \frac{\partial \Psi}{\partial X}\frac{\partial C}{\partial Y} = \frac{1}{Sc}\nabla^2 C \tag{9}$$

$$\text{where } Fc = \frac{1.75|\mathbf{v}|}{\sqrt{150} \times \epsilon^{\frac{3}{2}}} \quad \text{and } |\mathbf{v}| = \sqrt{\left(\frac{\partial \Psi}{\partial \mathbf{Y}}\right)^2 + \left(\frac{\partial \Psi}{\partial \mathbf{X}}\right)^2}$$

where T, C, ζ, Ψ, and τ are respectively non-dimensional temperature, concentration, vorticity, stream function, and time. The non-dimensional parameters that appear in the equations are $Gr_i^T = \frac{g\beta_i(\theta_h - \theta_c)^i L^3}{\nu^2}$; $i = 1, 2, 3, 4$, the thermal Grashof numbers, $Gr_5^C = \frac{g\beta_5(c_1 - c_2)L^3}{\nu^2}$, the solutal Grashof number, $Pr = \nu/\alpha = 13.67$, the Prandtl number, $Sc = \nu/D$, the Schmidt number, and $Da = K/L^2$, the Darcy number.

The initial and boundary conditions in the dimensionless form are

$$\begin{array}{llllll}
\tau = 0; & \Psi = 0 & \zeta = T = C = 0 & 0 \le X \le 1 & 0 \le Y \le 1 \\
\tau > 0; & \Psi = \frac{\partial \Psi}{\partial Y} = 0 & \frac{\partial T}{\partial X} = \frac{\partial C}{\partial X} = 0 & \text{at } X = 0\&1 & 0 \le Y \le 1 \\
 & \Psi = \frac{\partial \Psi}{\partial X} = 0 & T = 1, C = 0 & \text{at } Y = 0 & 0 \le X \le 1 \\
 & \Psi = \frac{\partial \Psi}{\partial X} = 0 & T = 0, C = 1 & \text{at } Y = 1 & 0 \le X \le 1
\end{array}$$

The local Nusselt number, which accounts for the rate of heat transfer across the enclosure is computed at hot wall and defined by $Nu = \frac{\partial T}{\partial Y}\big|_{Y=0}$, and the average Nusselt number is given by $\overline{Nu} = \int_0^1 Nu \, \mathrm{d}X$. The mass transfer rate across the enclosure is calculated by Sherwood number and defined by $Sh = \frac{\partial C}{\partial Y}\big|_{Y=1}$, and the average Sherwood number is given by $\overline{Sh} = \int_0^1 Sh \, \mathrm{d}X$.

3 Numerical method

The non-dimensional equations subject to the boundary conditions are integrated over a control volume as explained by Patankar (1980). The power-law scheme is used for the convection-diffusion formulation. The solution domain consists a number of grid points at which discretization equations are applied. The uniform grid has been selected in both X and Y directions. The grid size were tested from 21×21 to 101×101. It is observed from the grid independence test that a 41×41 uniform grid is enough to investigate the problem. The time step is chosen to be uniform $\Delta\tau = 10^{-4}$. The resulting algebraic equations for energy and vorticity are solved by Gauss–Seidel method whereas successive over relaxation (SOR) method is used to solve equation for stream function. Thus, having calculated the temperature and vorticity values at an advance point in time $\tau = (n + 1)\,\mathrm{d}\tau$, using their respective solution given at $\tau = (n)\,\mathrm{d}\tau$ (n=0 corresponds to the initial condition), the stream function is solved for its solution at this advanced time step. The resulting stream function values are then used to determine the velocity components and the boundary values of the vorticity. Thus, the sequence beginning with the solution of the energy equation is applied repeatedly until the desired accuracy of results are obtained. The convergence criterion used for the field variables $\phi (= T, C, \zeta, \Psi)$ is $\left|\frac{\phi_{(n+1)}(i,j) - \phi_{(n)}(i,j)}{\phi_{(n+1)}(i,j)}\right| \le 10^{-5}$.

Table 1 Calculated Grashof numbers for different hot wall temperatures

θ_h (K)	Gr_1	Gr_2	Gr_3	Gr_4	Gr_5
277	286885	168235	18333	1812	44205
278	358607	262868	35807	4423	47363
279	430328	378530	61875	9173	50520
280	502050	515221	98256	16995	53678
281	573771	672942	146668	28993	56835
281.5	609632	759688	175924	36949	58414
282	645493	851692	208831	46441	59993
283	717214	1051472	286462	70783	63150
284	788936	1272281	381282	103634	66308
285	860657	1514120	495007	146777	69465

4 Results and discussion

Buoyancy-driven convective flow in a square cavity filled with water saturated porous medium is studied numerically around the region of its density maximum. The Grashof numbers are calculated for different hot wall temperatures, $4°C \leq \theta_h \leq 12°C$, and displayed in Table 1. The investigations are carried out for various porosities, Darcy numbers and Grashof numbers. The results are depicted as streamlines, velocity vectors, isotherms, isoconcentrationlines, and velocity profiles. Figure 2a–f shows the fluid flow, heat, and mass transfer phenomena for $\epsilon = 0.2$, $Da = 0.1$, and different Grashof numbers. When $Gr_1 = 286885$ that is, $\Delta T = 4°C$, Fig. 2a, fluid density increases so that no density inversion effects occur in the enclosure, since the maximum density plane coincides with the hot wall, cool low density fluid rises along the cold wall while warm, higher density fluid descends along the hot wall. It is observed that a counter clockwise rotating cell occupied the whole cavity with $|\Psi| = 0.231$. It can be seen that the uniform mixing in the case of $Gr = 286885$. It slowly turns into a conduction type heat transfer and feeble thermal boundary layer existing at the left top and right bottom is appearing.

Increasing Grashof number the maximum density plane just moves from hot wall, Fig. 2b. The density inversion exists inside the cavity. The corners of hot wall are affected and three eddies are present. The flow pattern is altered by forming of two eddies in the top and bottom left corners of the cavity with the flow directed up along the hot wall. Increasing Grashof number to 573771, the clockwise convective cell on the left side has strengthen, Fig. 2c. When $Gr = 609632$, the density gradient is approximately symmetric with respect to the vertical mid plane. The flow consists of a symmetric counter rotating cell pattern with up flow of warm and cold fluid near the vertical hot and cold walls and down flow near the vertical mid plane of the cavity. This slowly improves into a conduction type heat transfer for the case $Gr = 609632$. This is clearly seen from the Fig. 2d. Further increasing Grashof number, the maximum density plane develops close to the cold wall. The clockwise rotating cell near the hot wall has grown substantially in size and strength and suppressed its counter part. A further increase in Grashof number brings in convection mode of heat transfer and introduces thermal boundary layer at the left bottom and right top of the cavity. It is clearly seen that a convection dominants over most of the cavity in which the isotherms are close to horizontal.

When $Gr_1 = 860657$, the streamlines show that the convective cell generated at the cold wall is gradually compressed into the lower right hand corner. This is clearly seen from the Fig. 2f. Two convective cells are separated by the $\Psi = 0$ plane at all times. The

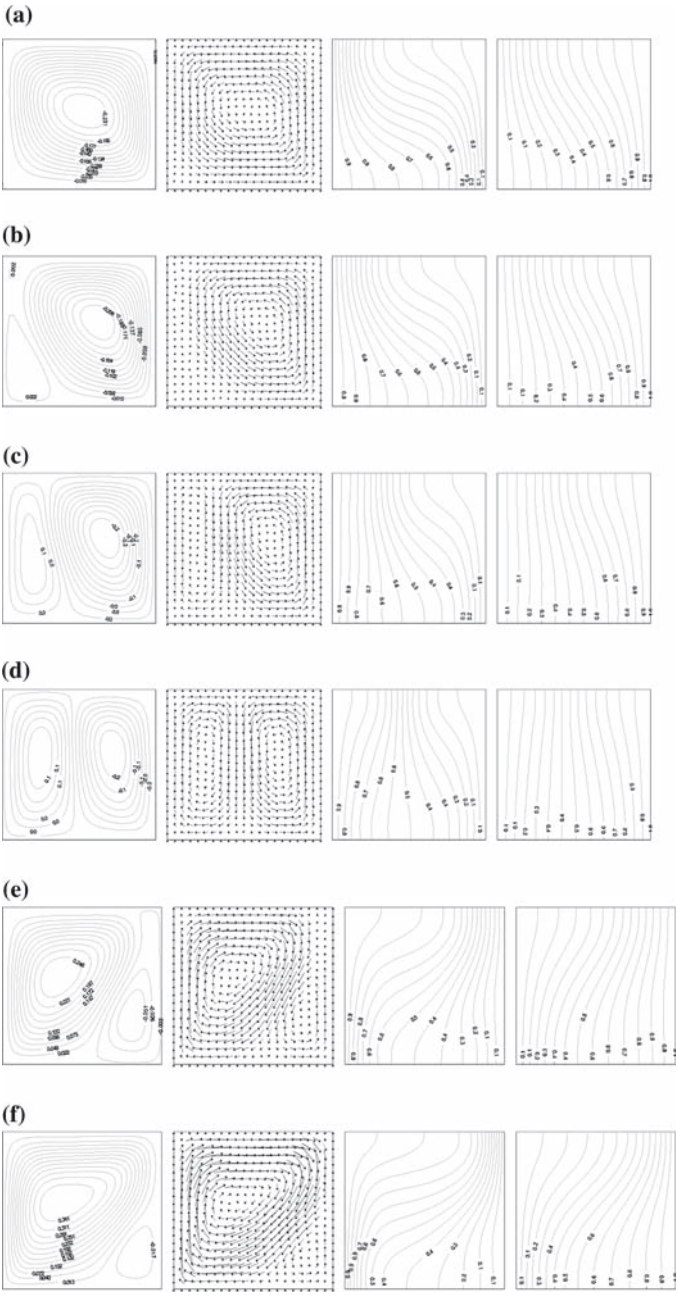

Fig. 2 (**a**) Streamlines, velocity vector, isotherms, concentration lines for $Gr_1 = 286885$, $\varepsilon = 0.2$ and Da = 0.1. (**b**) Streamlines, velocity vector, isotherms, concentration lines for $Gr_1 = 502050$, $\varepsilon = 0.2$ and $Da = 0.1$. (**c**) Streamlines, velocity vector, isotherms, concentration lines for $Gr_1 = 573771$, $\varepsilon = 0.2$ and $Da = 0.1$. (**d**) Streamlines, velocity vector, isotherms, concentration lines for $Gr_1 = 609632$, $\varepsilon = 0.2$ and $Da = 0.1$. (**e**) Streamlines, velocity vector, isotherms, concentration lines for $Gr_1 = 717214$, $\varepsilon = 0.2$ and $Da = 0.1$. (**f**) Streamlines, velocity vector, isotherms, concentration lines for $Gr_1 = 860657$, $\varepsilon = 0.2$ and $Da = 0.1$

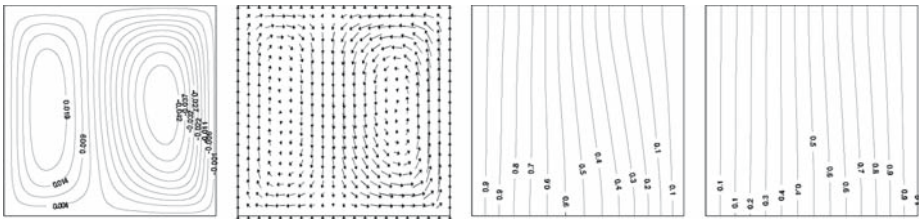

Fig. 3 Streamlines, velocity vector, isotherms, concentration lines for $Gr_1 = 573771$, $\varepsilon = 0.2$ and $Da = 0.01$

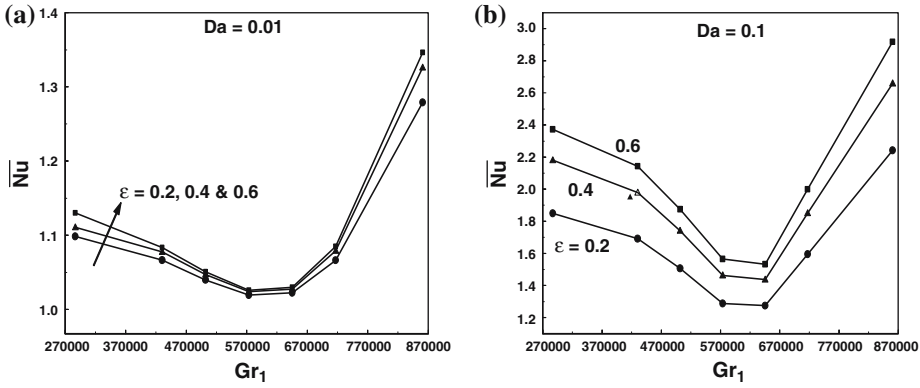

Fig. 4 Average Nusselt number for different porosities

configuration of the two counter rotating cells changing with the wall temperature affects the average heat transfer. The streamlines, velocity vector, isotherms, and concentrationlines for $Da = 0.01, \epsilon = 0.2$, and $Gr_1 = 573771$ are displayed in Fig. 3. When Da becomes 0.01 for all Grashof numbers a conduction type heat transfer flow phenomena is observed. The isotherms and concentration lines literally vertical indicate pure conduction type phenomena, which is natural in the case of almost equal counter rotating fluids. The circulation rate of the eddy $|\Psi| = 0.042$ is reduced compared to the previous case, $Da = 0.1$. This is because heat and mass transfer from one cell to another cell is purely by conduction since this is no transfer fluid from one cell to another.

The average Nusselt number for different porosities with $Da = 0.1$ and 0.01 are displayed in Fig. 4a, b. It is found that increasing the porosity increases the heat transfer rate for all Darcy numbers. It is noted from these figures that for a given porosity, average Nusselt number reaches a minimum about $Gr_1 = 600000$, this is because of the fact that an equally occupying bi-cellular flow pattern and pure conduction which is a slow mode of heat transfer resulting in the minimum of average Nusselt number. For such a situation, the dual cell structure inhibits the direct convective transfer of energy from the hot to the cold wall. This phenomenon results essentially from the inversion of the fluid density at 4°C and is one of its most significant effects on the mechanism of heat transfer by convection within a cavity. So heat transfer rate is reduced in such a situation for all values of Darcy numbers. The variation of average Nusselt number for a given Da among different porosity is high in the case of $Da = 0.1$ than $Da = 0.01$. The effect of Darcy numbers on heat transfer is displayed in Fig. 5. It is clearly seen from the figure that the heat transfer rate is increased for increasing

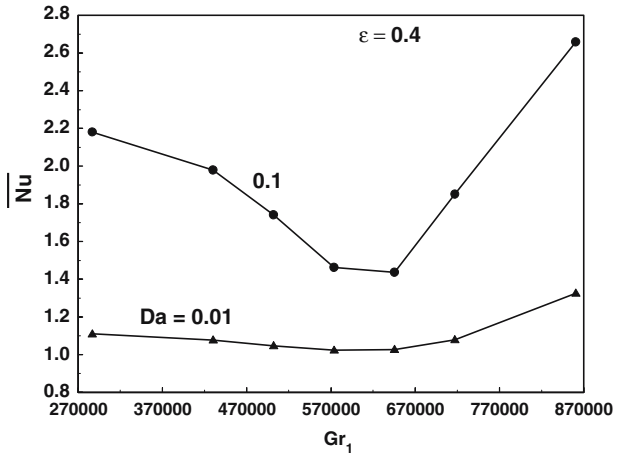

Fig. 5 Average Nusselt number for different Darcy numbers

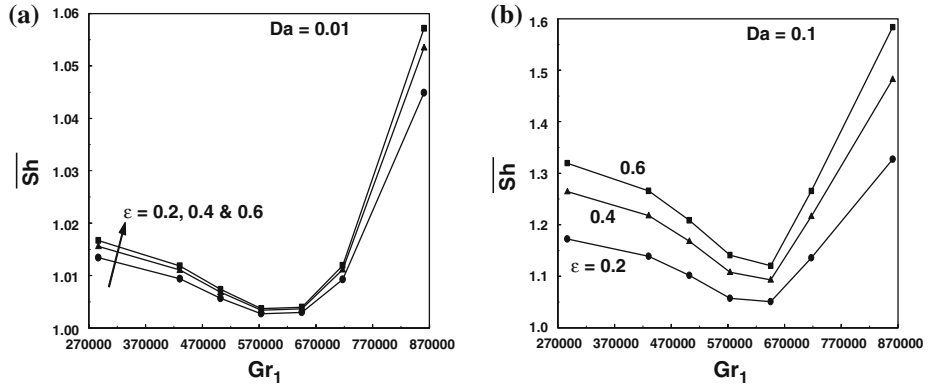

Fig. 6 Average Sherwood number for different porosities

Darcy number. The behavior in Fig. 4 for density inversion is also observed in the Fig. 5 for a given Darcy number.

The average Sherwood number for different porosity with $Da = 0.1$ and 0.01 are displayed in Fig. 6a, b. It is observed that increasing the porosity increases the mass transfer rate. It is noted from these figures that the variation of average Sherwood number for a given Da for different porosities is high when Darcy number is high. A similar behavior is observed for Sherwood number as in average Nusselt number, in Fig. 6a, b. The physical reasoning given for heat transfer above holds hood mass transfer too. The effect of Darcy numbers on mass transfer is displayed in Fig. 7. The mass transfer rate is increased by increasing Darcy number. Figures 5 and 7 clearly indicate a fall in heat transfer (average Nusselt number value) and fall in mass transfer (average Sherwood number value) as Da decreases. This is purely because a decrease in Da leads to minimum space available in the porous matrix for the flow and hence heat and mass transfer.

Figure 8 shows the time history of the average Nusselt number for various Grashof numbers. As time evolves the particles near the hot wall have higher temperature and so the heat

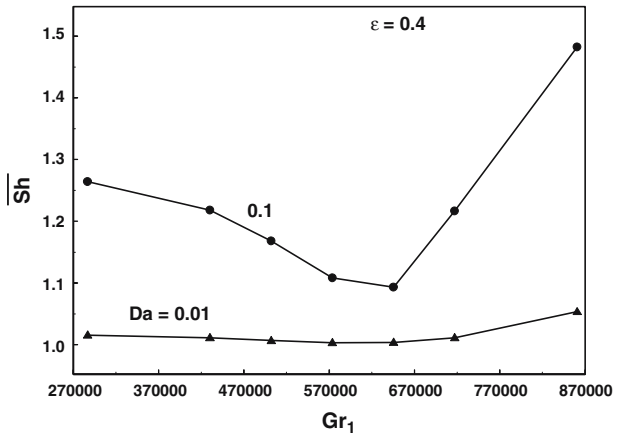

Fig. 7 Average Sherwood number for different Darcy numbers

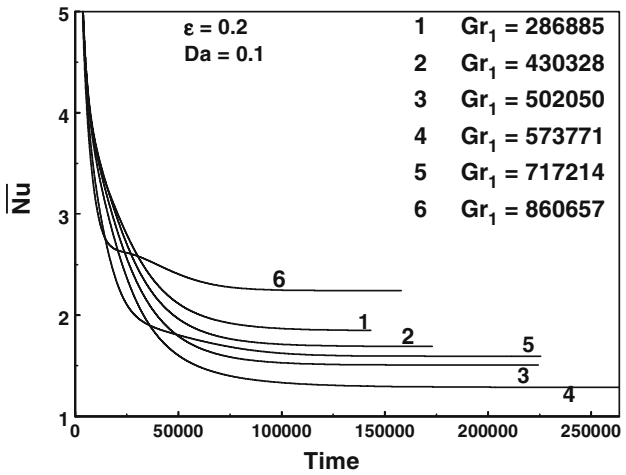

Fig. 8 Time history of average Nusselt number for different Grashof numbers

transfer rate starts decreasing, thus, we get a sudden fall in the values of $\overline{Nu}$ as seen in the graph. Finally, the steady state is reached and the $\overline{Nu}$ tends to be constant. For increasing the Grashof number the heat transfer rate first decreases and then increases, which contradicts the fact that heat transfer rate is increased with Grashof number, because of the reason the inversion of the fluid density at 4°C. Figure 9 shows the time history of the average Sherwood number for various Grashof numbers. The mass transfer rate also behaves like heat transfer rate.

Midheight velocity profiles for different Grashof numbers are depicted in the Fig. 10. The bidirectional velocity curves clearly shows the dual cell structure. Figure 11 shows the mid-height velocity profile for different porosities. It is noted that increasing the porosity increases the velocity of the fluid particles inside the cavity.

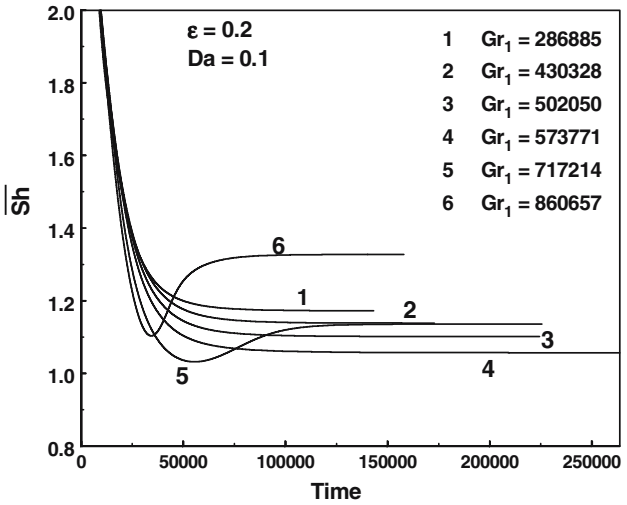

Fig. 9 Time history of average Sherwood number for different Grashof numbers

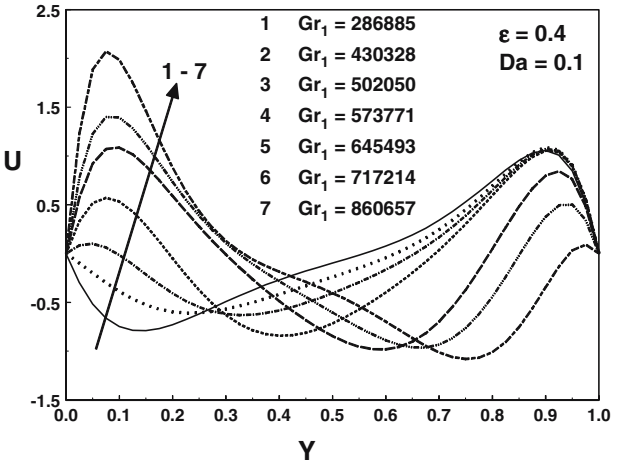

Fig. 10 Mid-height velocity for different Grashof numbers

5 Conclusion

The effects of density maximum of water on fluid flow, heat and mass transfer have been studied for different combination of parameters. It is observed that the temperature of maximum density leaves strong effects on heat and mass transfer due to the formation of bicellular structure. The non-linear behavior of heat and mass transfer rate are also because of the maximum density effect. The results show that higher heat and mass transfer rates can be achieved in a water saturated porous medium in the presence of high porosity. The heat and mass transfer rates are found to increase with increasing Darcy number.

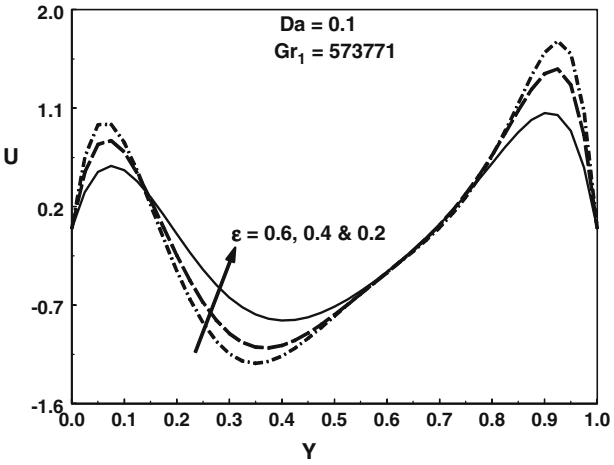

Fig. 11 Mid-height velocity for different porosities

Acknowledgements The third author would like to thank the Research Grants Council of the Honk Kong Special Administrative region, China, for their financial support through Project No. HKU 7192/04E.

References

Barbir, F.: PEM fuel cells: theory and practice. Elsevier Academic Press (2005)

Benhadji, K., Robillard, L., Vasseur, P.: Convection in a porous cavity saturated with water near 4°C and subject to Dirichlet–Neumann thermal boundary conditions. Int. Commun. Heat Mass Transfer **29**, 897–906 (2002)

Gobin, D., Bennacer, R.: Double diffusive natural convection in aqueous solutions near the density maximum. Int. Commun. Heat Mass Transfer **23**, 971–982 (1996)

Goyeau, B., Songbe, J.P., Gobin, D.: Numerical study of double-diffusive natural convection in a porous cavity using the Darcy–Brinkman formulation. Int. J. Heat Mass Transfer **39**, 1363–1378 (1996)

Ho, C.J., Lin, Y.H.: Natural convection of cold water in a vertical annulus with constant heat flux on the inner wall. J. Heat Transfer **112**, 117–123 (1990)

Kandaswamy, P., Kumar, K.: Buoyancy-driven nonlinear convection in a square cavity in the presence of a magnetic field. Acta Mech. **136**, 29–39 (1996)

Khanafer, K., Vafai, K.: Double-diffusive mixed convection in a lid-driven enclosure filled with a fluid saturated porous medium. Numerical Heat Transfer Part A **42**, 465–486 (2002)

Lin, D.S., Nansteel, M.W.: Natural convection in a vertical annulus containing water near the density maximum. J. Heat Transfer **109**, 899–905 (1987)

Mamou, M., Vasseur, P., Bilgen, E.: Multiple solution for double-diffusive convection in a vertical porous enclosure. Int. J. Heat Mass Transfer **38**, 1787–1798 (1995)

Mehta, K.N., Nandakumar, K.: Natural convection with combined heat and mass transfer buoyancy effects in non-homogeneous porous medium. Int. J. Heat Mass Transfer **30**, 2651–2656 (1987)

Nield, D.A., Bejan, A.: Convection in porous media. Springer (2006)

Nithiarasu, P., Sundararajan, T., Seetharamu, K.N.: Double-diffusive natural convection in a fluid saturated porous cavity with a freely convecting wall. Int. Commun. Heat Mass Transfer **24**, 1121–1130 (1997)

Patankar, S.V.: Numerical heat transfer and fluid flow. Hemisphere, McGraw-Hill, Washington, DC (1980)

Poulikakos, D.: Maximum density effects on natural convection in a porous layer differentially heated in the horizontal direction. Int. J. Heat Mass Transfer **27**, 2067–2075 (1984)

Sivasankaran, S., Kandaswamy, P.: Double diffusive convection of water in a rectangular partitioned enclosure with temperature dependent species diffusivity. Int. J. Fluid Mech. Res. **33**(4), 345–361 (2006)

Sundaravadivelu, K., Kandaswamy, P.: Double diffusive non-linear convection in square cavity. Fluid Dyn. Res. **27**, 291–303 (2000)

Sunden, B., Faghri, M.: Transport phenomena in fuel cells. WIT Press, Southampton, Boston (2005)

Vafai, K.: Handbook of porous media, 2nd edition, Marcel Dekker Inc. (2005)
Vasseur, P., Robillard, L., Chandra Shekar, B.: Natural convection heat transfer of water within a horizontal cylindrical annulus with density inversion effects. J. Heat Transfer **105**, 117–123 (1983)
Weiss, D.W., Stickler, L.A., Stewart , W.E. Jr.: The effect of water density extremum on heat transfer within a cylinder containing a heat-generating porous media. Int. Commun. Heat Mass Transfer **18**, 259–271 (1991)
Zheng, W., Robillard, L., Vasseur, P.: Convection in a square cavity filled with an anisotropic porous medium saturated with water near 4°C. Int. J. Heat Mass Transfer **44**, 3463–3470 (2001)